Electronic Supplementary Information for

Chemical state changes of Nafion in model polymer electrolyte fuel cell under oxygen/hydrogen gas atmosphere observed by S-K XANES spectroscopy

Kazuhisa Isegawa[a], Daehyun Kim[a], and Hiroshi Kondoh*[,a]

[a]Department of Chemistry, Keio University, 3-14-1 Hiyoshi, Kohoku-ku, Yokohama, Japan.

*To whom correspondence should be addressed.

E-mail: kondoh@chem.keio.ac.jp

Index **Page**

1. Cyclic voltammetry curves for the MEAs depending on humidity

Figure S1 and S2 show cyclic voltammetry (CV) curves for the MEAs under the condition indicated in the figure. For example, "wet, -0.2 V" means that the MEA was kept under a wet gas-flowing condition at a cathode voltage of -0.2 V vs. SHE. Each CV curve was recorded for a potential range from -0.05 to 1.00 V at a scan rate of 50 mV/s with keeping the humidity unchanged. The hydrogen adsorption peak (0.2-0.4 V) has moved to the higher potential side than literatures because of the fast sweep rate. Comparison of the CV curves shown in Figure S2 indicates that the conductivity is not completely recovered after the MEAs were once exposed to an overdried condition for a long time, even though returning to the wet condition. This is most likely due to adsorption of sulfur on platinum catalysts on the anode, as described in the text, in addition to other deterioration phenomenon of platinum catalyst and Nafion.

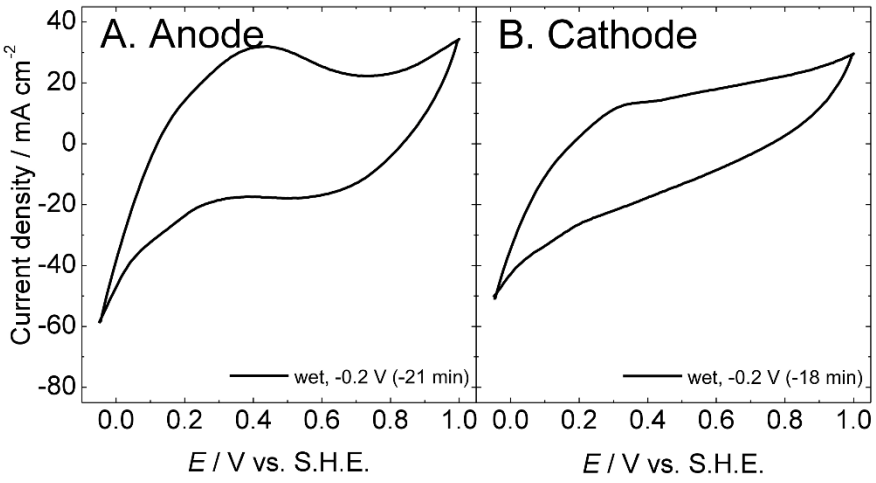

Figure S1. Cyclic voltammetry (CV) curves for the MEAs under wet gas-flowing conditions: (A) anode side, (B) cathode side. The measurement time corresponds to that in fig. 2 in the main text. All the CV curve measurements were conducted at a scan rate of 50 mV/s.

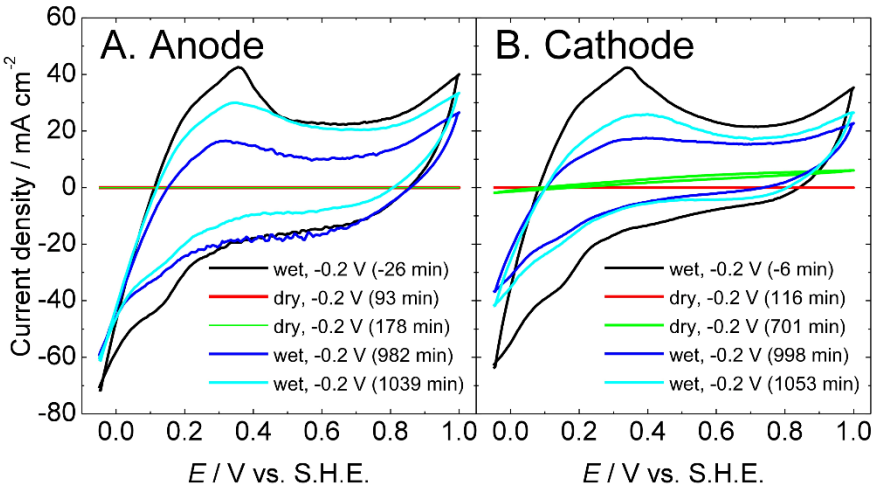

Figure S2. Cyclic voltammetry (CV) curves for the MEAs under wet and dry gas-flowing conditions: (A) anode side, (B) cathode side. The measurement time corresponds to that in fig. 6 in the main text. All the CV curve measurements were conducted at a scan rate of 50 mV/s.

2. Open circuit voltage changes due to humidity and temperature

Changes in open circuit voltage and temperature of model PEFCs during the experiment of changing humidity under oxygen gas-flowing conditions are shown in Figure S3. The apparent open circuit potential changes depending on the experimental condition, although the electrode reaction does not proceed under the present conditions. The reason for this is assumed that the standard hydrogen electrode itself is affected by humidity changes.

Changes in open circuit voltage and temperature of model PEFCs during the experiment of supplying oxygen gas onto the sulfur-poisoned catalyst are shown in Figure S4. Changes in the open circuit potential due to humidity were detected similarly to those in Figure S3. In (2) region of Figure S3, it takes time to lower the apparent open circuit voltage, but in (2) region of Figure S4, the apparent open circuit voltage increased as soon as the wet fuel gases were introduced. This tendency is consistent with the report that sulfonic acid groups dehydrate gradually but hydrate in a short time. [1,2]

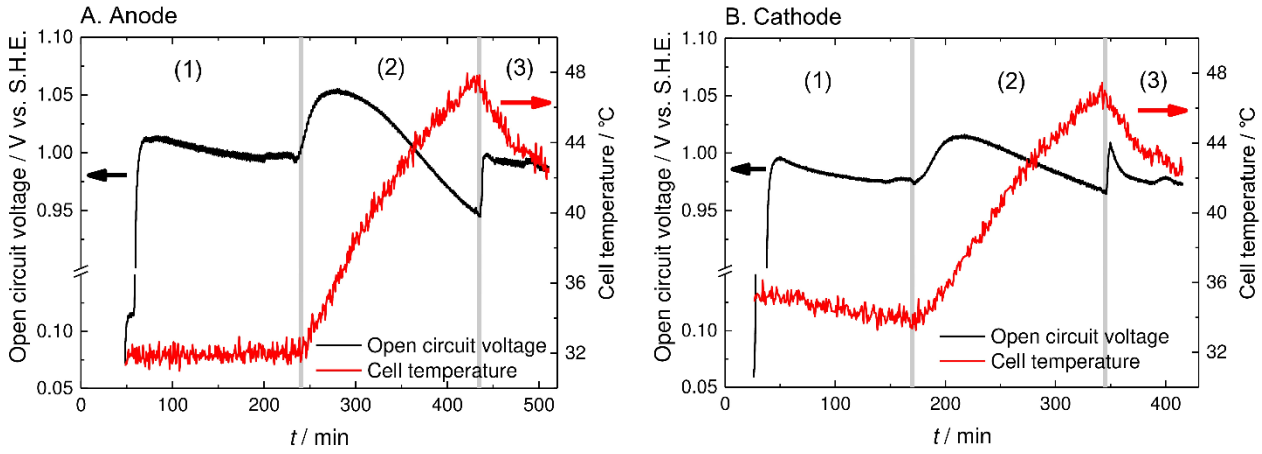

Figure S3. Change in open circuit voltage and temperature of PEFCs under $He+O_2/H_2$ gas-flowing conditions: (A) anode side, (B) cathode side. The measurement time corresponds to that in fig. 2. Operating conditions for each region are as follows: (1) no heating of the cell with supplying humidified $He+O_2/H_2$, (2) heating of the cell with supplying dry $He+O_2/H_2$, (3) no heating of the cell with supplying humidified $He+O_2/H_2$.

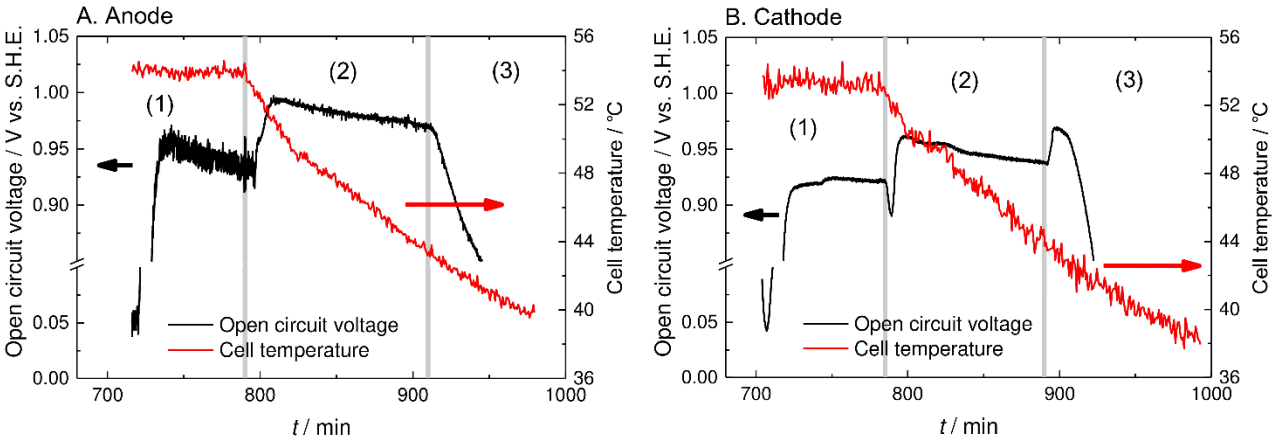

Figure S4. Change in open circuit voltage and temperature of PEFCs under $He+O_2/H_2$ gas-flowing conditions: (A) anode side, (B) cathode side. The measurement time corresponds to that in fig. 6. Operating conditions for each region are as follows: (1) heating of the cell with supplying dry $He+O_2/H_2$, (2) no heating of the cell with supplying humidified $He+O_2/H_2$, (3) no heating of the cell with supplying humidified He/H_2.

3. Peak analysis of low-energy region of the S-K XANES spectra

In this section, we discuss whether the 2471.1 eV peak (atomic sulfur on platinum)[3,4] and the 2473.7 eV peak (thioether group)[5,6] behave independently or not.

Figure S5 shows an enlarged view of the low energy region of Fig. 2, where wet or dry He+O_2/H_2 gases were flown. On the anode electrode, the spectral curves appear convex upward at 2471.1 eV even for the first spectrum. This indicates that the MEA is already sulfur-poisoned during the break-in operation under reducing atmosphere (H_2 gas-flowing). On the other hand, on the cathode electrode, the first spectrum appears convex downward at 2471.1 eV when He is supplied during the break-in operation. Furthermore the spectral curves for the cathode remain similar under any conditions used afterward because reduction of sulfonic acid is suppressed by oxidizing atmosphere (He+O_2 gas-flowing).

Figure S6 shows intensity changes of the peak at 2471.1 eV and the peak at 2473.7 eV. In Figure S6A, the two components exhibit different behaviors. In Figure S6B, the plots of the peak at 2473.7 eV fluctuate significantly, particularly for wet oxygen flowing (blue plot), compared to those of the 2471.1 eV peak, which suggests the 2473.7 eV peak behaves independently of the 2471.1 eV peak.

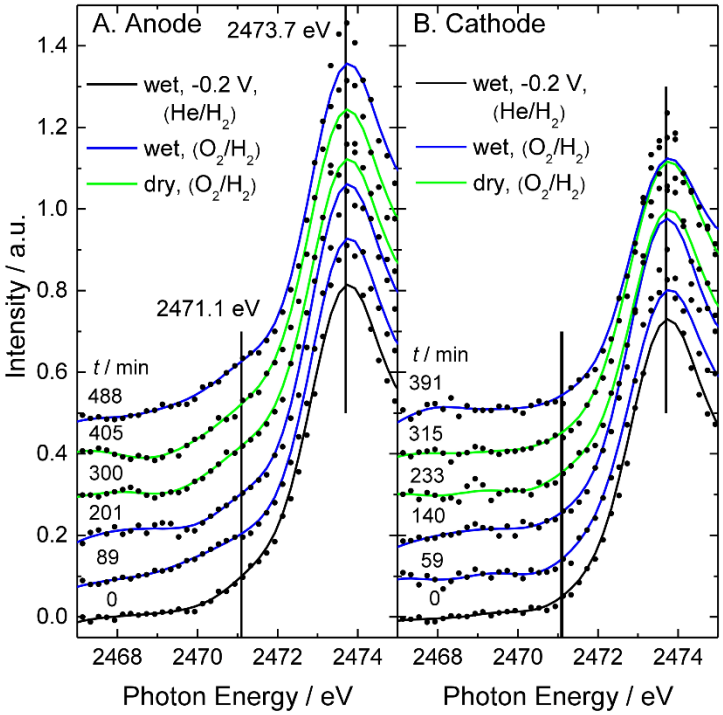

Figure S5. Low-energy region of the S-K XANES spectra taken under gas-flowing conditions shown in Fig. 2 on a magnified scale (dots: observed points, solid lines: smoothed curves), where wet and dry He+O_2/H_2 gases were flown after the break-in operation. The elapsed time from the initial measurement is shown at the left-hand side. The vertical lines correspond to the energy positions where the atomic sulfur adsorbed on Pt (2471.1 eV) and impurity thioether (2473.7 eV). The color code is the same as that in Fig. 2.

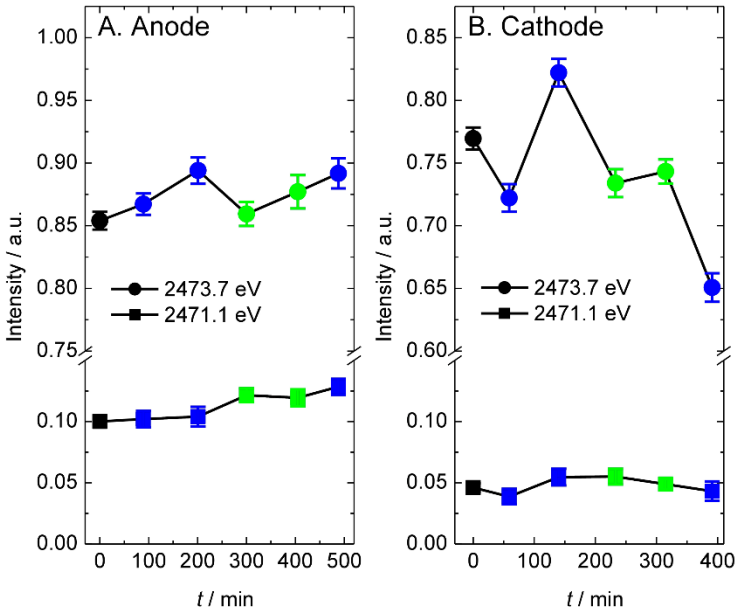

Figure S6. Plots of the intensity averaged over 5 points around 2471.1 eV and 2473.7 eV of the XANES spectra shown in Fig. 2 as a function of elapsed time. The color code is the same as that in Fig. 2.

Figure S7 shows an enlarged view of the low energy region of Fig. 5, where dry He/H_2 gases were first flown and then dry and wet $He+O_2/H_2$ gases were subsequently flown. The 2471.1 eV peak is increased with time on the anode electrode. On the other hand, on the cathode electrode the 2471.1 eV peak becomes larger exclusively under dry condition and reduces by the introduction of oxygen gas.

Figure S8 shows plots of the intensity changes of the 2471.1 eV and 2473.7 eV peaks. In Figure S8A, the peak at 2473.7 eV once reduces and then increases, while the 2471.1 eV peak exhibits a continuously increasing tendency. In Figure S8B, the intensity of the peak at 2473.7 eV keeps unchanged except for the blue plot. As mentioned before, the behavior of the blue plot may be caused by fluctuation during wet oxygen flowing. Thus, no clear correlation is observed between the 2471.1 eV and 2473.7 eV peaks and they seem to behave independently. Therefore, it is most likely that the thioether species included in the carbon support does not influence on poisoning of the platinum catalyst.

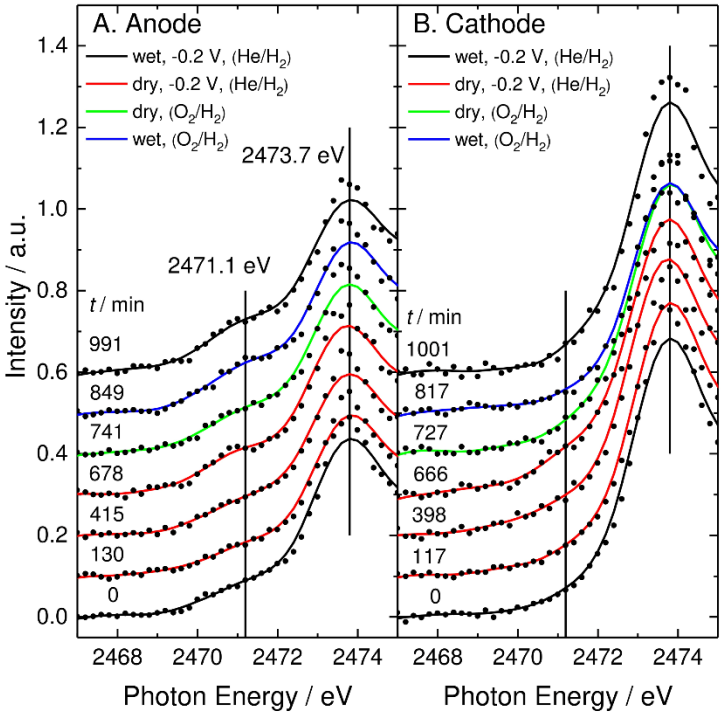

Figure S7. Low-energy region of the S-K XANES spectra taken under gas-flowing conditions shown in Fig. 5 on a magnified scale (dots: observed points, solid lines: smoothed curves), where dry He/H_2 gases were flown after the break-in operation and then dry and wet $He+O_2/H_2$ gases were subsequently flown. The elapsed time from the initial measurement is shown at the left-hand side. The vertical lines correspond to the energy positions where the atomic sulfur adsorbed on Pt surfaces (2471.1 eV) and impurity thioether (2473.7 eV). The color code is the same as that in Fig. 5.

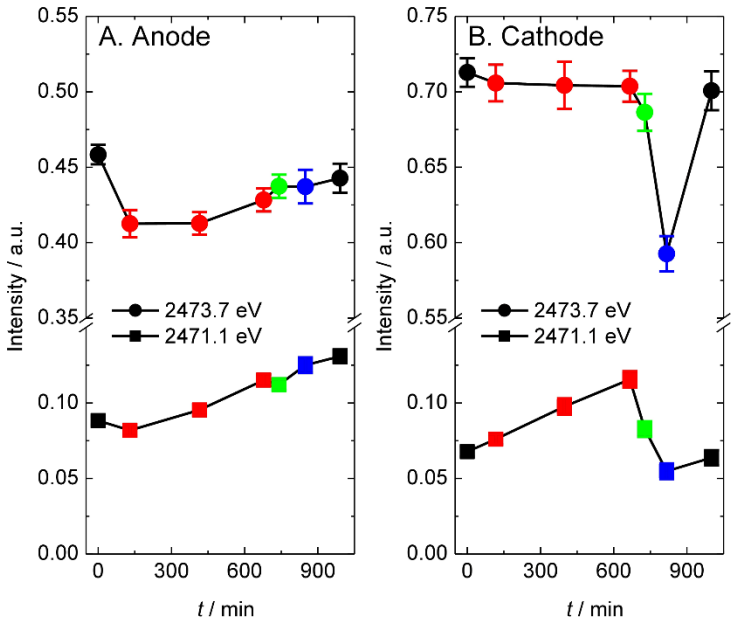

Figure S8. Plots of the intensity averaged over 5 points around 2471.1 eV and 2473.7 eV of the XANES spectra shown in Fig. 5 as a function of elapsed time. The color code is the same as that in Fig. 6.

References

1. K. Kunimatsu, B. Bae, K. Miyatake, H. Uchida and M. Watanabe, *J. Phys. Chem. B*, 2011, **115**, 4315-4321.
2. T. Shimoaka, C. Wakai, T. Sakabe, S. Yamazaki and T. Hasegawa, *Phys. Chem. Chem. Phys.*, 2015, **17**, 8843-8849.
3. O. A. Baturina, B. D. Gould, A. Korovina, Y. Garsany, R. Stroman and P. A. Northrup, *Langmuir*, 2011, **27**, 14930-14939.
4. O. A. Baturina, B. D. Gould, P. A. Northrup and K. E. Swider-Lyons, *Catal. Today*, 2013, **205**, 106-110.
5. J. Prietzel, J. Thieme, U. Neuhäusler, J. Ssusini and I. Kögel-Knabner, *Eur. J. Soil Sci.*, 2003, **54**, 423-433.
6. F.-R. Orthous-Daunay, E. Quirico, L. Lemelle, P. Beck, V. deAndrade, A. Simionovici and S. Derenne, *Earth. Planet. Sci. Lett.*, 2010, **300**, 321-328.